

## INVESTIGATION OF SOLAR CELLS FABRICATED ON n-TYPE SUBSTRATES

Wan Zulhafizhazuan, Cheow Siu Leong, Suhaila Sepeai,  
K. Sopian and Saleem H. Zaidi

*Solar Energy Research Institute (SERI), Universiti Kebangsaan Malaysia  
43600 UKM Bangi, Selangor, Malaysia*

*Corresponding author: wanzulhafizhazuan@gmail.com*

### ABSTRACT

In comparison with p-doped wafers, the n-doped wafer offers advantages in terms of superior tolerance to impurities and lack of light induced degradation. Recent defect studies on solar cell have also determined a higher tolerance of chemical and crystallographic defects in n-type wafer. In addition, the solar cells fabricated on n-type wafers are less susceptible to shunt especially in high efficiency solar cells which require shallow emitters. In this paper, n<sup>+</sup>np<sup>+</sup> solar cell configuration has been modelled using commercially available PC1D resulting in efficiency of 19.56 %. With identical processing conditions based on conventional POCl<sub>3</sub>-emitter formation. Preliminary solar cell LIV measurements exhibit efficiencies of 5.51 % and 9.44 % for n and p-doped wafers, respectively.

*Keywords: Si solar cells; n-type wafers; Crystalline Si; POCl<sub>3</sub> emitter; PC1D simulation; Aluminum back surface field;*

### INTRODUCTION

Tremendous efforts by researchers in terms of publication have been expanded on the optimization of energy conversion from sunlight into electricity by solar cells since sun represents truly universal green and free source of energy. A review of the worldwide production of solar cells reveals that almost 95 % is traced to Silicon [1]. In terms of market share, the boron doped Si wafer represents almost 95 % in comparison with the phosphorus-doped Si wafer [2]. However, future prospects for the n-type silicon wafer appear bright since several international companies such as Panasonic and LG have been reported in initiating production based on n-wafer solar cells [3]. In addition, in excess of 20 % efficiencies on n wafer solar cells have been reported by SunPower Inc. and Sanyo [4]. During the early phase of photovoltaic (PV) cell industrialization, the manufacturing technology was driven by need for improvements for aerospace applications such in satellites. Boron-doped wafer solar cells were preferred by aerospace industry due to its superior lifetime. Consequently, the terrestrial PV market was also dominated by the p-type substrate solar cells[3]. Field research has revealed that p type wafer solar cell suffers from light-induced degradation (LID) and has lower

tolerance to impurities, therefore its performance is degraded [5]. In contrast, the n-type wafer solar cell is free from boron-oxygen complexes and exhibits higher tolerance to impurities thus resulting in longer carrier lifetimes, which leads to higher efficiencies. A case study, based on photo conductance lifetime monitoring, on impact of water contamination on n and p wafer solar cells indicated that n type wafer solar cell was largely unaffected by contamination in comparison with the p type wafer solar cell even after it was processed in contaminated diffusion and oxidation furnaces [4]. Therefore, n-wafer solar cells help to eliminate recombination associated with contamination.

## EXPERIMENTAL

### *PC1D Simulation*

Commercially available PC1D software was used to model performance of n wafer solar cell in terms of critical solar cell parameters such as bulk conductivity, front surface field and minority carrier lifetime [6]. Figure 1 describes a schematic diagram of the modelled solar cell configuration. This model simulation was carried out for 100-cm<sup>2</sup> area n type silicon solar cell with fixed series resistance, shunt conductance and 200- $\mu$ m wafer thickness. With regards to optical characteristics, pyramidal texture was assumed with fixed properties 10 % front surface reflectance. Base contact and internal conductor were set at 0.0015  $\Omega$  and 0.3 S respectively [7]. Optimized solar cell efficiencies as high as 19.56 % were achieved. Bulk conductivity concentrations were varied in 1.513E11/cm<sup>3</sup> to 1.513E16/cm<sup>3</sup> range. The front surface field doping concentration was varied from 1.27E18/cm<sup>3</sup> to 1.27E21/cm<sup>3</sup>. The minority carrier lifetime was varied from 0.001  $\mu$ s to 1000  $\mu$ s. Finally, the front surface recombination velocity was varied in 1E6 cm/s to 100 cm/s.

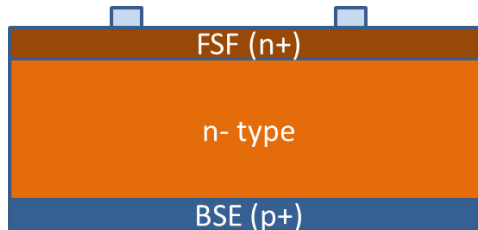


Figure 1: Cross-sectional configuration of the n-type wafer solar cell

### *Solar Cell Fabrication*

Five-inch square with area about 156.25 cm<sup>2</sup> n and p-type Si wafers at 200- $\mu$ m thickness were etched in 10 % NaOH solutions for 10 minutes at 70 °C to remove wire saw damage. Wafer orientations were (100) with bulk minority carrier lifetime specified at 10  $\mu$ s. Damage-removed wafers were subjected to texturing process to form pyramidal structure in conventional KOH, isopropyl alcohol (IPA) and de-ionized (DI) water (H<sub>2</sub>O) solution at 70 °C. Following texturing and cleaning processes, n and p-type wafers were thermally oxidized to form about 500-nm thick oxide films. Prior to phosphorus diffusion in POCl<sub>3</sub> furnace, front surface oxide was etched off. Phosphorous diffusion was carried out at 875 °C, and a thermally grown oxide film was used for passivation and anti-reflection coating. Following diffusion and oxidation steps, back

surface oxide was removed and screen printing of Ag on front and Al on the rear surface was carried out. Screen-printed contacts were co-fired in RTC 615 six-zone furnace. The performance of fabricated solar cells was evaluated by dc mode solar cell tester with xenon light source; an eighteen percent commercially-manufactured solar cell was used for calibration. The dc mode solar cell tester measures critical solar cell parameters including open-circuit voltage, short-circuit current, fill factor, series resistance, shunt resistance, and efficiency.

## RESULTS AND DISCUSSION

### PCID Simulations

#### Bulk Resistivity Analysis

Doping concentration in the silicon substrate plays an important role in determining solar cell performance. Bulk resistivity variation also leads to respective changes in wafer conductivity and minority carrier lifetime. In this simulation, doping concentration was varied in  $1.513\text{E}14/\text{cm}^3$  to  $1.513\text{E}16/\text{cm}^3$  range for which the calculated resistivity increased from  $0.3717 \Omega.\text{cm}$  to  $292 \Omega.\text{cm}$ ; remaining solar cell parameters were kept fixed. Simulation results plotted in Figure 2 reveal that efficiency is constant over broad range. However, it drops rapidly to zero at  $1.513\text{E}16/\text{cm}^3$ . This can be attributed to a sensitive relationship between bulk doping concentration and minority carrier lifetime; lifetime decreases rapidly as the bulk concentration increases beyond a critical limit. This is further illustrated in solar cell efficiency variation with lifetime discussed in the following sections. The typical value of bulk resistivity for phosphorous-doped wafer in industrial environment is in  $0.5 \Omega.\text{cm}$  to  $3 \Omega.\text{cm}$  range. From simulations in Figure 2 the bulk concentration value of  $1.513\text{E}15/\text{cm}^3$  represents  $3 \Omega.\text{cm}$  wafer resistivity.

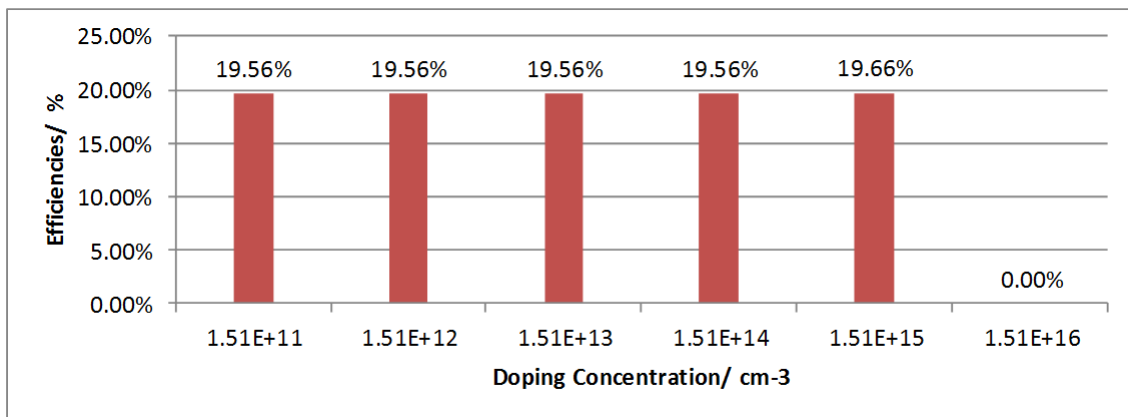


Figure 2: Efficiency variation as a function of the bulk resistivity

#### Front Surface Field

The performance of the n-dope wafer solar cell as a function of doping concentration is plotted in Figs. 3-6. Front surface field (FSF) doping concentration was varied in

$1.27E18/cm^3$  to  $1.27E21/cm^3$  range. These values are well within experimentally attainable values through appropriate control of process parameters such as temperature, time, and gas flow rate during diffusion process. From the plotted data, similar behaviour is observed for open-circuit voltage ( $V_{OC}$ ), short-circuit current ( $I_{SC}$ ), fill factor (FF), and efficiency (Eff). There is slow reduction in all three parameters as doping concentration is increased over three orders of magnitude. At the highest doping concentration of  $1.27E21/cm^3$ , steep performance reduction is noted (Figure 6).

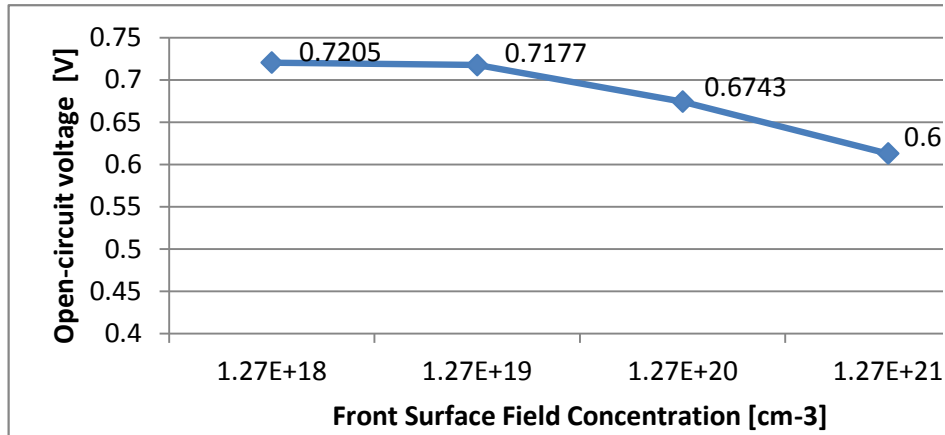


Figure 3: Open-circuit voltage variation with FSF concentration

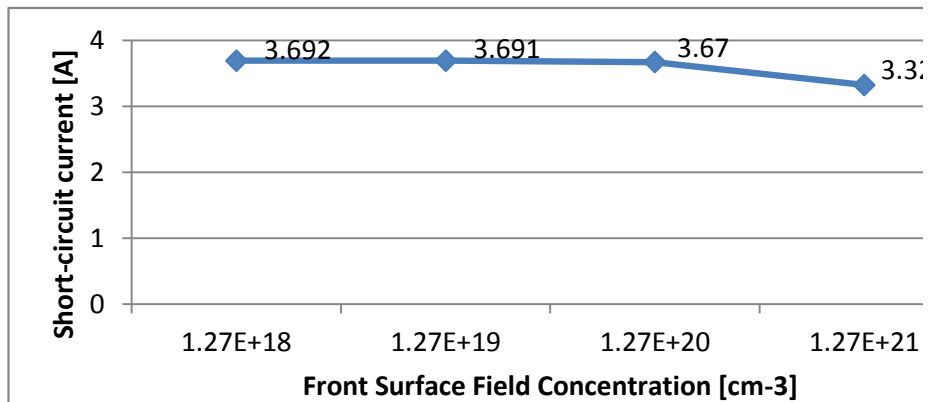


Figure 4: Short-circuit current variation with FSF concentration

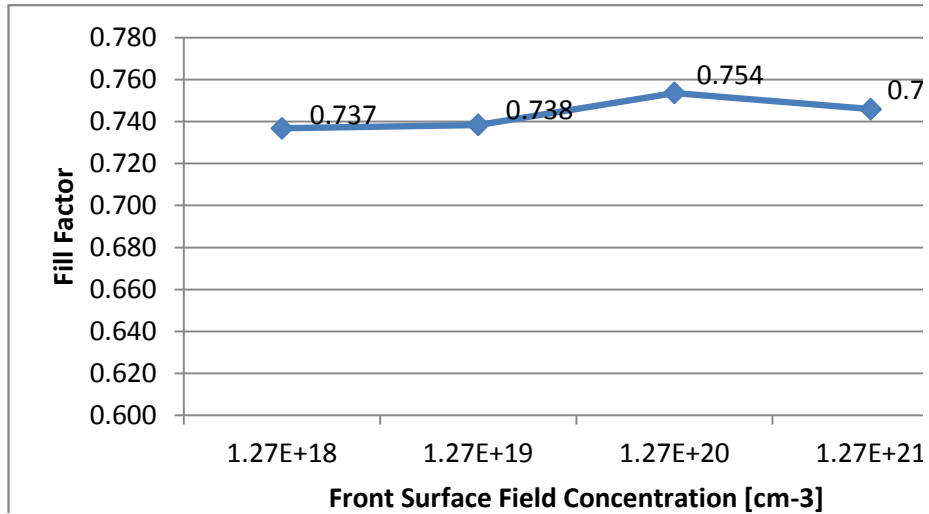


Figure 5: Fill Factor variation with FSF concentration

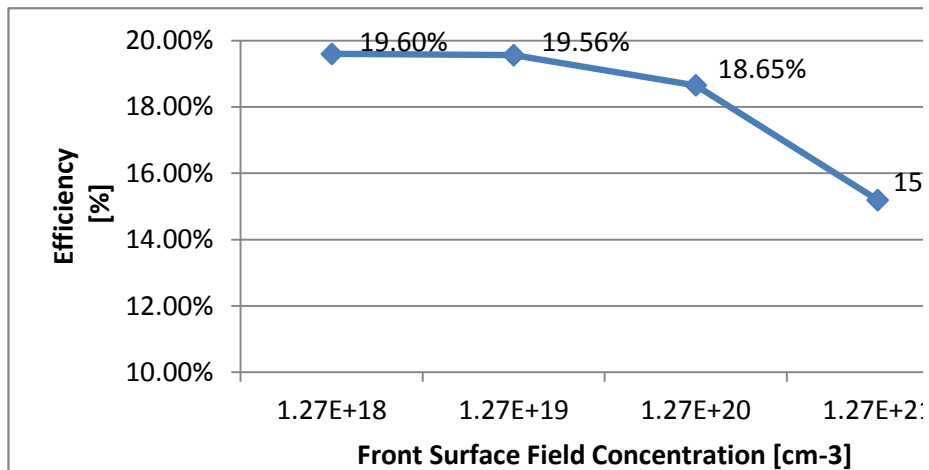


Figure 6: Efficiency variation with FSF concentration

*Front Surface Recombination Velocity.*

Figures 7-9 display relationship between efficiency, open circuit voltage, and short-circuit current as a function of front surface recombination. The front surface recombination velocity was varied from 1E2cm/s to 1E6cm/s. Solar cell efficiency (Figure 7) was reduced from ~ 19.53 % at 100 cm/s to 12.71 % at 1E6 cm/s. High recombination losses at the front surface, where majority of photo-generated e-h pairs are created, are responsible for steep performance degradation. Therefore, superior surface passivation at the front solar cell surface is required for higher efficiencies.

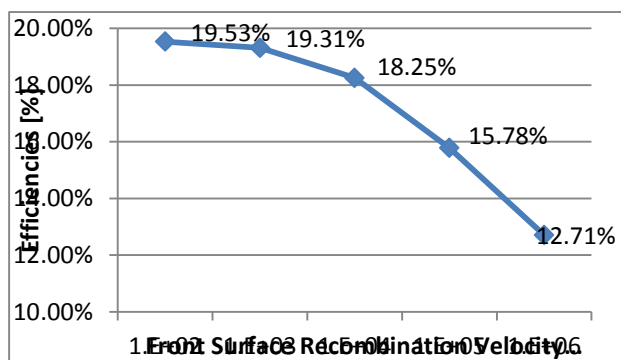


Figure 7: Efficiency variation with front surface recombination velocity

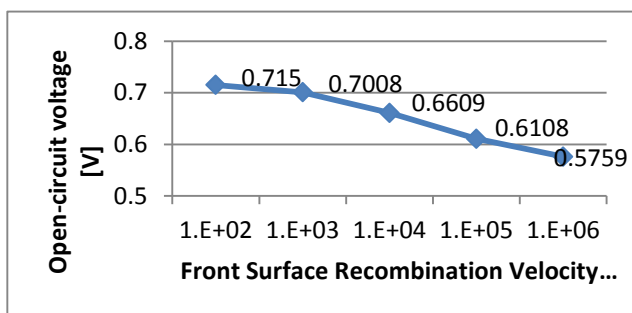


Figure 8: Open-circuit voltage variation with front surface recombination velocity

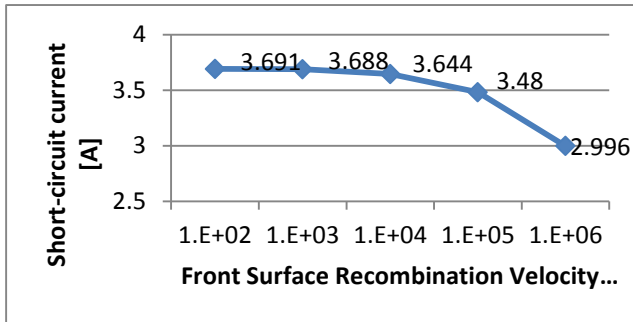


Figure 9: Short-circuit current variation with front surface recombination velocity

*Minority Carrier Lifetimes*

Solar cell performance was evaluated as a function of minority carrier lifetime from 0.001 μs to 1000 μs; all other solar cell parameters were kept fixed. Figures 10-13 plot  $V_{OC}$ ,  $I_{SC}$ , FF, and efficiency as a function of minority carrier lifetime. All four parameters behave in a similar fashion with negligible performance at 0.001 μs to near saturation levels at about 500 μs. This behaviour can be explained in terms of electron-hole pair diffusion across the 200-μm thickness of the solar cell. Diffusion length is related to lifetime by the equation (1).

$$L_{DIFF} = \text{sqrt}(\tau * D) \tag{1}$$

Where  $\tau$  is the minority carrier lifetime in seconds and  $D$  is the Si diffusivity in  $\text{m}^2/\text{sec}$ ;  $D = 8.8\text{E-}5 \text{ m}^2/\text{sec}$  for crystalline Si. Therefore, at  $\tau = 0.001 \mu\text{s}$ ,  $L_{DIFF} = 0.3 \mu\text{m}$  which is 667 times smaller than the wafer thickness, therefore, a major fraction of e-h pairs are likely to be lost to recombination. In contrast, at  $\tau = 500 \mu\text{s}$ ,  $L_{DIFF} = 210 \mu\text{m}$ , which is larger than wafer thickness, therefore, only an infinitesimal fraction of e-h pairs will be lost to recombination.

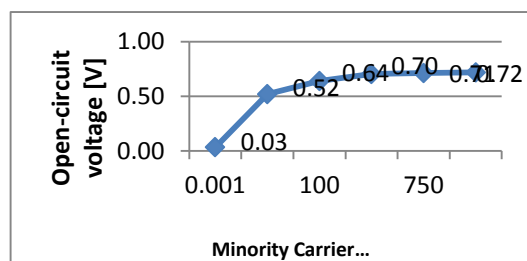


Figure 10: Open-circuit voltage variation with minority carrier lifetime

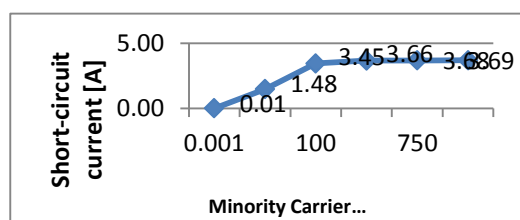


Figure 11: Short-circuit current variation with minority carrier lifetime

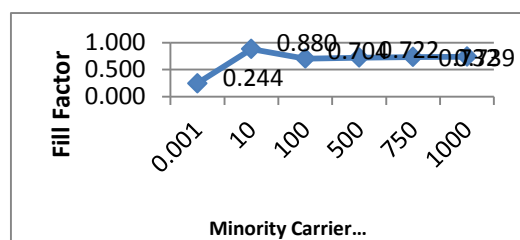


Figure 12: Fill factor variation with minority carrier lifetime

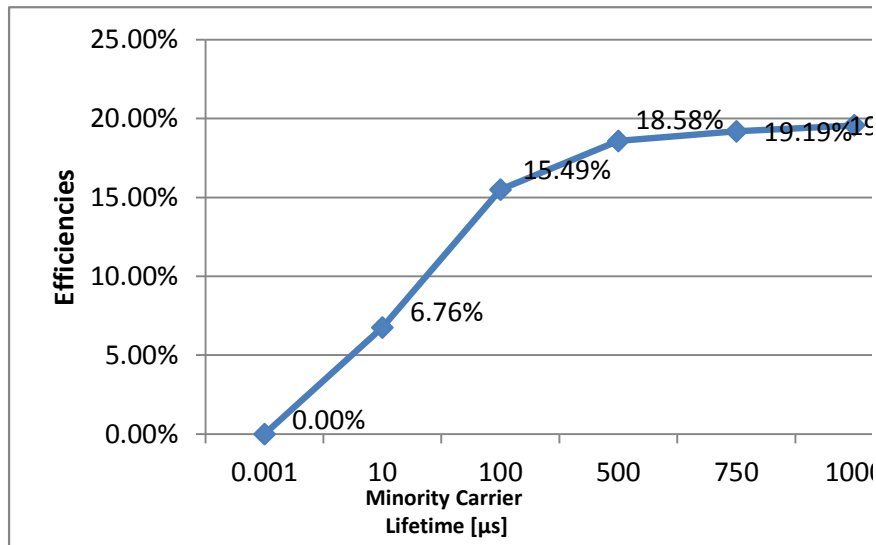


Figure 13: Efficiency variation with minority carrier lifetime

#### *Fabrication Results*

Figure 14 plots light current-voltage (LIV) measurements at AM 1.5 illumination for solar cells fabricated on both n and p type substrates; the LIV response from 18 % efficiency commercial solar cell is also included as baseline reference. Table 1 summarizes key solar cell parameters. In Figure 14, the reference solar cell expectedly exhibits the highest efficiency in comparison with the n and p wafer solar cells at UKM/SERI facilities. This lack of higher performance can be attributed to poor minority carrier lifetimes and high surface recombination velocities of both p and n wafers. Based on PC1D simulations (Figure 10), good agreement is noted with predicted efficiency of about 5 % for lifetime of 10- $\mu$ sec. The efficiency of p-doped wafer solar cell is almost twice as much due to the presence of emitter on the front surface. The front surface emitter field facilitates collection large fraction of light-generated e-h pairs prior to recombination. In contrast, the n-doped wafer solar cell has junction field at the rear surface, and a majority of the e-h pairs are lost to recombination prior to separation by junction electric field, hence high lifetime wafers are required for n-type wafer based solar cell.

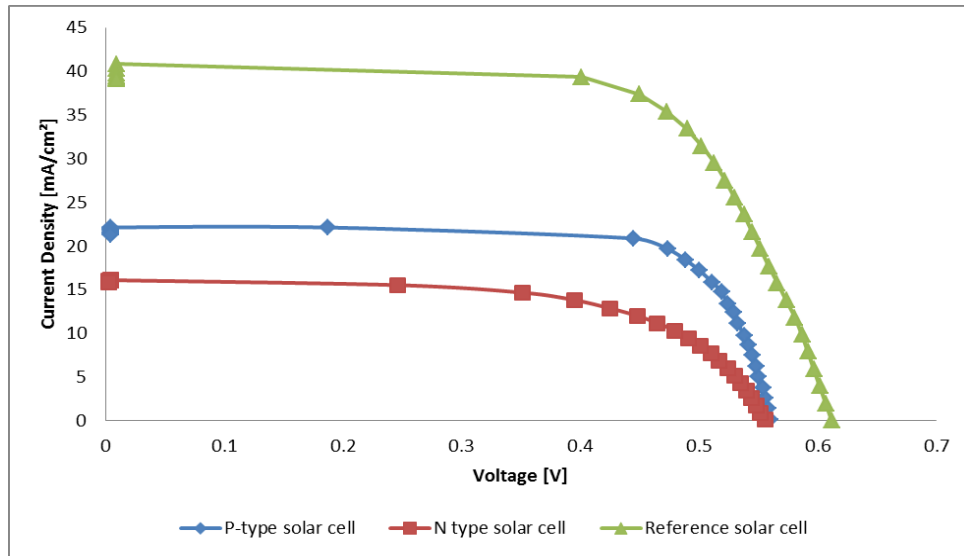


Figure 14: LIV response of solar cells under AM 1.5 illumination

Table 1: Performance variations of n and p wafer solar cells

| Performances             | Reference Cell | n- wafer Solar Cell | p-wafer solar cell |
|--------------------------|----------------|---------------------|--------------------|
| Voc [V]                  | 0.612          | 0.56                | 0.56               |
| Jsc [A/cm <sup>2</sup> ] | 0.041          | 0.017               | 0.02               |
| FF                       | 0.671          | 0.604               | 0.7467             |
| Series Resistant [Ohm]   | 0.241          | 0.970               | 0.5512             |
| Shunt Resistance [Ohm]   | 7.0            | 12.41               | 23.5               |
| Efficiency [%]           | 18.0           | 5.51                | 9.44               |

## CONCLUSION

A detailed simulation of solar cells fabricated in n-type wafer has been carried out. Conventional industrial monofacial solar cell manufacturing solar process based on p-doped wafer was applied to n-type wafers. Preliminary solar cell fabrication results indicate higher efficiency from the p-doped wafer solar cell due to poor minority carrier and surface passivation lifetime. High lifetime and superior surface passivation are required to fabricate high efficiency solar cells.

## ACKNOWLEDGEMENTS

The author would like to acknowledge various financial supports from PRGS/1/13/TK07/UKM/01/1, ERGS/1/2013/TK07/UKM/01/1, FRGS/1/2014/SG02/UKM/03/1, and AP 2013-010.

## REFERENCES

- [1]. N. Asim, K. Sopian, S. Ahmadi, K. Saeedfar, M. a. Alghoul, O. Saadatian, S. H. Zaidi, *Renew. Sustain. Energy Rev.* **16** 5834–5847 (2012)
- [2]. R. Burgers, R. C. G. Naber, J. J. Carr, P. C. C. Barton, L. J. J. Geerligs, X. Jingfeng, G. Li, S. Weipeng, H. An, Z. Hu, P. R. Venema, a H. G. Vlooswijk, *25th Eur. Photovolt. Sol. Energy Conf. Exhib.* 1106–1109 (2010)
- [3]. <http://www.pvtech.org>
- [4]. J. E. Cotter, J. H. Guo, P. J. Cousins, M. D. Abbott, F. W. Chen, K. C. Fisher, *IEEE Trans. Electron Devices* **53** 1893–1901 (2006)
- [5]. J. Schmidt and R. Hezel, *12th Work. Cryst. Silicon Sol. Cell Mater. Process.* 1–8 (2002)
- [6]. <https://www.engineering.unsw.edu.au>
- [7]. S. Sepeai, S. H. Zaidi, M. K. M. Desa, M. Y. Sulaiman, N. a Ludin, M. A. Ibrahim, and K. Sopian, *J. Energy Technol. Policy* **3** 1–11 (2013)